Title: Marine biomarkers from ice cores reveal enhanced high-latitude Southern Ocean carbon sink during the Antarctic Cold Reversal

This is a non-peer reviewed EarthArXiv pre-print in review in *Global Change Biology*

Title: Marine biomarkers from ice cores reveal enhanced high-latitude Southern Ocean carbon sink during the Antarctic Cold Reversal

Authors: C.J. Fogwill*[1,2], C.S.M. Turney[2,3,4], L. Menviel[4], A. Baker[2], M. E. Weber[5], B. Ellis[6], Z.A. Thomas[2,3,4], N. R. Golledge[7,8], D. Etheridge[9], M. Rubino[1,9,10], D.P. Thornton[9], T.D. van Ommen[11,12], A.D. Moy[11,12], M.A.J. Curran[11,12], S. Davies[13], M.I. Bird [3,14], N.C. Munksgaard[14,15], C.M. Rootes[16], H. Millman[1,4], J. Vohra[2], A. Rivera[17], A. Mackintosh[18], J. Pike[19], I.R. Hall[19], E.A. Bagshaw[19], E. Rainsley[1], C. Bronk Ramsey[20], M, Montinari[1], A. Cage[1], M. Harris[1], R. Jones[21†], A. Power[21], J. Love[21], J. Young[22], L.S. Weyrich [3,22], A. Cooper[3,22]

Affiliations:

[1]School of Geography, Geology and the Environment, University of Keele, Staffordshire, UK

[2]Palaeontology, Geobiology and Earth Archives Research Centre, School of Biological Earth and Environmental Sciences, University of New South Wales, 2052, Australia

[3]ARC Centre of Excellence in Australian Biodiversity and Heritage

[4]Climate Change Research Centre, School of Biological Earth and Environmental Sciences, University of New South Wales, 2052, Australia

[5]Steinmann Institute, University of Bonn, Poppelsdorfer Schloss, Bonn, Germany

[6]Research School of Earth Sciences, Australian National University, Canberra, Australia

[7]Antarctic Research Centre, Victoria University of Wellington, Wellington 6140, New Zealand

[8]GNS Science, Lower Hutt, 5001, New Zealand

[9]CSIRO Oceans and Atmosphere, Aspendale, Victoria, 3195 Australia

[10]Dipartimento di Matematica e Fisica, Università della Campania "Luigi Vanvitelli", viale Lincoln, 5-81100 Caserta, Italy

[11]Department of the Environment, Australian Antarctic Division, 203 Channel Highway, Kingston, Tasmania 7050, Australia

[12]Antarctic Climate & Ecosystems Cooperative Research Centre, University of Tasmania, Private Bag 80, Hobart, Tasmania 7001, Australia

[13]Department of Geography, Swansea University, Swansea, United Kingdom

[14]Centre for Tropical Environmental and Sustainability Science, College of Science, Technology and Engineering, James Cook University, Cairns, Australia

[15]Research Institute for the Environment and Livelihoods, Charles Darwin University, Australia

[16]Department of Geography, University of Sheffield, United Kingdom

[17]Glaciology and Climate Change Laboratory, Centro de Estudios Cientficos, Valdivia, Arturo Prat 514, Chile

[18]School of Earth, Atmosphere and Environment, Monash University, Melbourne, Australia

[19]School of Earth and Ocean Sciences, University of Cardiff, Wales, UK

[20]Research Laboratory for Archaeology and the History of Art, University of Oxford, Dyson Perrins Building, South Parks Road, Oxford, OX1 3QY, UK

[21] BioEconomy Centre, The Henry Wellcome building for Biocatalysis, Biosciences, Stocker Road, Exeter University, Exeter, EX4 4QD, UK

[22]Australian Centre for Ancient DNA, University of Adelaide, 5005, Australia

Contact Information: *Correspondence to c.j.fogwill@keele.ac.uk

Abstract: The Southern Ocean plays a fundamental role in regulating global atmospheric CO_2 levels, yet the underlying processes and feedbacks that control the carbon cycle today remain unclear. The Last Glacial Transition (LGT 18,000-11,000 years ago or 18-11 kyr BP) experienced rapid and sustained changes in CO_2 that may provide fresh insights, however, fundamental questions over the mechanism(s) that modulate climate-carbon dynamics during this important period remain. One key example is the enigmatic 1,900-year plateau that interrupted the rise in atmospheric CO_2 during the LGT during a period of pronounced mid- to high-latitude Southern Hemisphere cooling termed the Antarctic Cold Reversal (ACR, 14,600-12,700 years ago or 14.6-12.7 kyr BP). Here we utilise five independent approaches to provide a detailed marine biomarker reconstruction from a highly-resolved Antarctic 'horizontal' ice core. Our reconstruction provides a coherent signal of enhanced surface ocean productivity and microbial diversity, in the form of marine picoeukaryotes and nanoplankton, that have been captured within ice from precipitation derived from the South Atlantic sector of the high-latitude Southern Ocean. When combined with marine sediment records, we confirm this period was coincident with increased biological export (driving CO_2 sequestration), suggesting high-latitude biological feedbacks contributed to the ACR CO_2 plateau. Transient climate modelling indicates that this period coincided with the maximum seasonal variability in sea-ice extent, implying sea-ice feedbacks enhanced CO_2 sequestration, making the high-latitude South Atlantic sector Southern Ocean a significant carbon sink that contributed to the sustained plateau in CO_2 levels during the ACR. This finding has ramifications for our understanding of contemporary ice-ocean-carbon feedbacks, and confirms the dynamic role Antarctic sea ice plays, providing a negative feedback during periods of rising CO_2, a result that requires detailed assessment given recent

88 **high-latitude sea ice changes, that may impact the efficiency of the Southern Ocean carbon**
89 **sink.**

90 **Introduction:** The Southern Ocean occupies some 14% of the planet's surface and plays a
91 fundamental role in the global carbon cycle and climate (Bauska et al., 2016; Le Quéré et al., 2007;
92 Marshall and Speer, 2012). It provides a direct connection to the deep ocean carbon reservoir
93 through physical and biological processes that include surface primary productivity,
94 remineralisation of carbon at depth, and upwelling of carbon-rich and radiocarbon (^{14}C)-depleted
95 water masses (Gottschalk et al., 2016; Marshall and Speer, 2012; Turney et al., 2016). However,
96 the role of these different processes in modulating past and future air-sea carbon flux remains
97 poorly understood (Hewitt et al., 2016; Schmitt et al., 2012). Considerable uncertainty surrounds
98 the source(s) and sink(s) of carbon during the Last Glacial Termination (LGT; 19 to 11.6 kyr BP)
99 when atmospheric CO_2 rose from approximately 190 parts per million (ppm) to around 270 ppm
100 (Figure 1). Recent detailed analysis of the stable isotopic composition of atmospheric carbon
101 dioxide ($\delta^{13}C$-CO_2) from Antarctic ice cores provides new insights into the potential effects of
102 terrestrial carbon in defining rapid rises in CO_2, but highlighted that CO_2 variability across this
103 period may reflect a combination of sources, sinks and feedbacks (Bauska et al., 2016), that may
104 provide valuable insights into the role of the Southern Ocean processes in modulating global CO_2
105 today (Barnes, 2015).

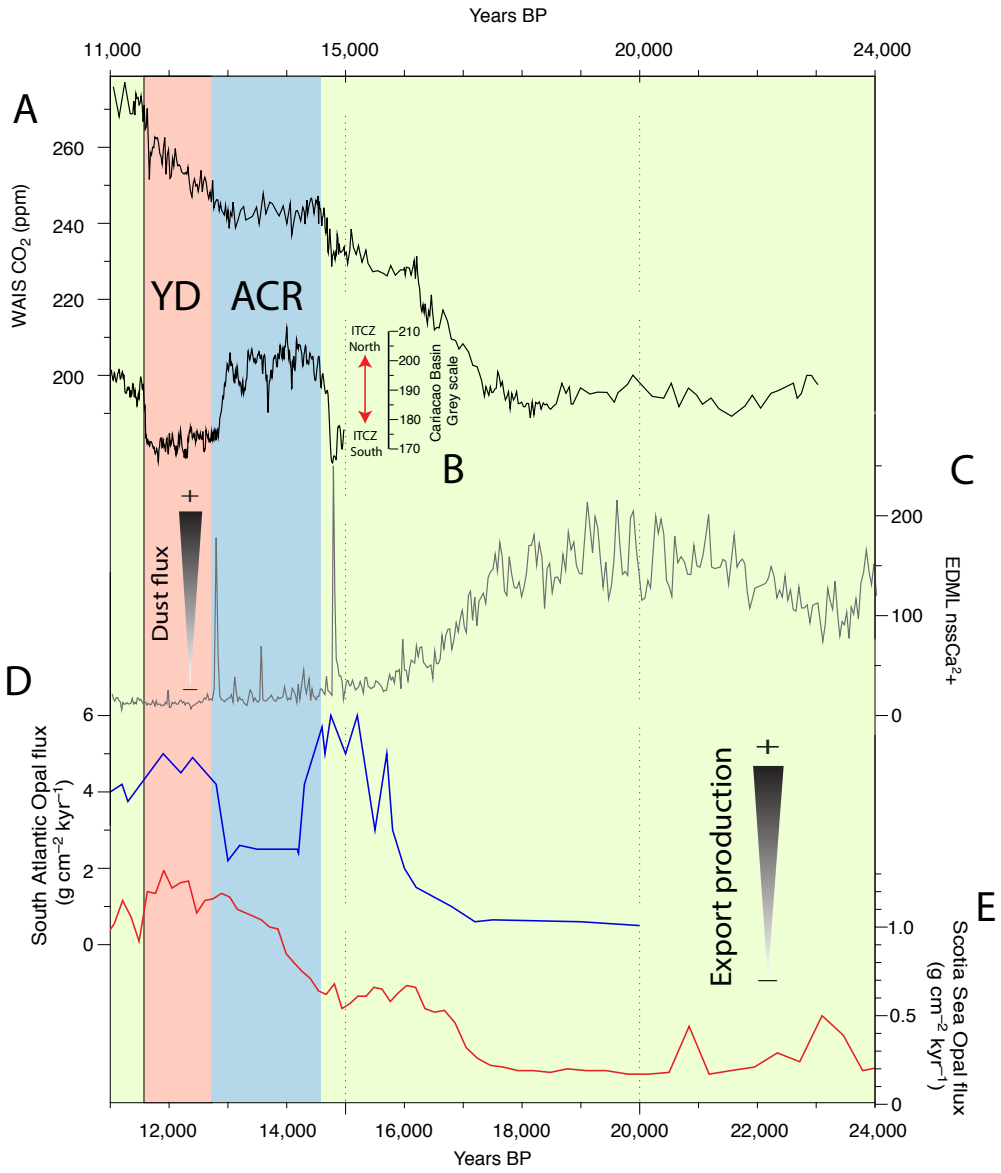

Figure 1. Comparison of A. Atmospheric CO_2 concentration from the WAIS divide core (WD_{2014} chronology) (Marcott et al., 2014) with available Southern Hemisphere records of B. Cariaco Basin grey scale, a measure of latitudinal changes in the trade winds associated with the ITCZ (Hogg et al., 2016). C. non-sea salt Ca^{2+} flux (nssCa2+) from EPICA Dronning Maud Land (EDML) (Wolff et al., 2006a). D. South Atlantic opal flux from core TN057-13 (Anderson et al., 2009). E. Scotia Sea opal flux from core MD07-3134 (Weber et al., 2014). Vertical boxes indicate the periods defined by the Antarctic Cold Reversal (ACR) (blue), the Younger Dryas (YD)

chronozone (11.7-12.7 kyr BP).

The parallel changes in Antarctic temperature and atmospheric CO_2 have been interpreted as climate playing a substantial role in the carbon budget of the Southern Ocean (Anderson et al., 2009; Monnin et al., 2001). Several physical and biological mechanisms have been invoked to explain these observations. These include changes in the strength and/or latitudinal migration of the mid-latitude Southern Hemisphere jet stream and prevailing surface westerly air flow that drives Southern Ocean overturning (Anderson et al., 2009; Marshall and Speer, 2012; Toggweiler et al., 2006), variations in iron (dust) fertilization of subantarctic phytoplankton impacting the efficiency of the Southern Ocean biological carbon pump (Jaccard et al., 2016; Jaccard et al., 2013; Martínez-García et al., 2014), Antarctic sea-ice controlling CO_2 exchange (Butterworth and Miller, 2016; Delille et al., 2014) and carbon drawdown (Barnes, 2015), as well as the potential impacts of a warming ocean on CO_2 exchange (Bauska et al., 2016). The role of the Southern Ocean as a source or sink of atmospheric carbon during the LGT remains highly contested, with the above processes not fully accounting for the pattern of change in CO_2 recorded over this period (Jaccard et al., 2016), implying that one or more mechanisms are currently not captured in our present understanding.

One striking feature of the LGT record is a 1,900 year-long-plateau in CO_2 concentration, when CO_2 paused at a near-constant 240 ppm coinciding with the period of high latitude Southern Hemisphere surface cooling, termed the Antarctic Cold Reversal (ACR; 14.6-12.7 kyr BP) (Pedro et al., 2015). Whilst the rapid rises in CO_2 may be attributed to either terrestrial carbon feedbacks or through shifts in the Intertropical Convergence Zone (ITCZ) that may have impacted ocean

circulation and the location and intensity of the Southern Hemisphere Westerlies (Bauska et al., 2016), the enigmatic plateau between 14.6-12.7 kyr BP remains unexplained (Figure 1). In the absence of clear mechanisms the need for well resolved palaeo-proxy reconstructions that may shed light on causes of this plateau are needed, as it may help reveal new insights into the high-latitude ocean's potential for carbon sequestration (Boyd et al., 2019). Here we exploit an innovative new ice core record to reconstruct high-latitude environmental changes during the ACR to gain new insights into the driver (s) of Southern Ocean carbon feedbacks during this important transition.

The ACR was characterized by surface cooling across the mid to high-latitude Southern Hemisphere (Fogwill and Kubik, 2005; McGlone et al., 2010; Pedro et al., 2015), coincident with sustained warming across the Northern Hemisphere (the North Atlantic Bølling-Allerød interstadial) (Jaccard et al., 2016; Marcott et al., 2014), abrupt global sea level rise (Fogwill et al., 2017; Weber et al., 2014), and major disruptions to atmospheric and ocean circulation, and the carbon cycle (Jaccard et al., 2016; Martínez-García et al., 2014; Schmitt et al., 2012). Whilst the global sequence of events during the ACR is reasonably well known (Pedro et al., 2015), a clear understanding of the drivers and impacts of contrasting polar climate changes on global CO_2 trends has proved elusive due to the challenges in precisely aligning ice and marine records across this period (Jaccard et al., 2016). In part this reflects the lack of well-resolved, high accumulation marine sedimentary records from the high-latitude Southern Ocean. One crucial record in this regard comes from marine sediment core TN057-13 (~53°S) (Anderson et al., 2009; Jaccard et al., 2016) (Figure 2), which suggests that the ACR was characterized by reduced carbon sequestration in the mid-latitudes (as measured by decreased biological productivity or export production

(Anderson et al., 2009; Gottschalk et al., 2016); Figure 1D), possibly the result of enhanced stratification that decreased the vertical supply of nutrients across the high-nutrient, low-chlorophyll (HNLC) sectors of the Southern Ocean during cooling (Anderson et al., 2009). However, such a hypothesis is difficult to test in the absence of other well resolved, high-latitude records of Southern Ocean productivity.

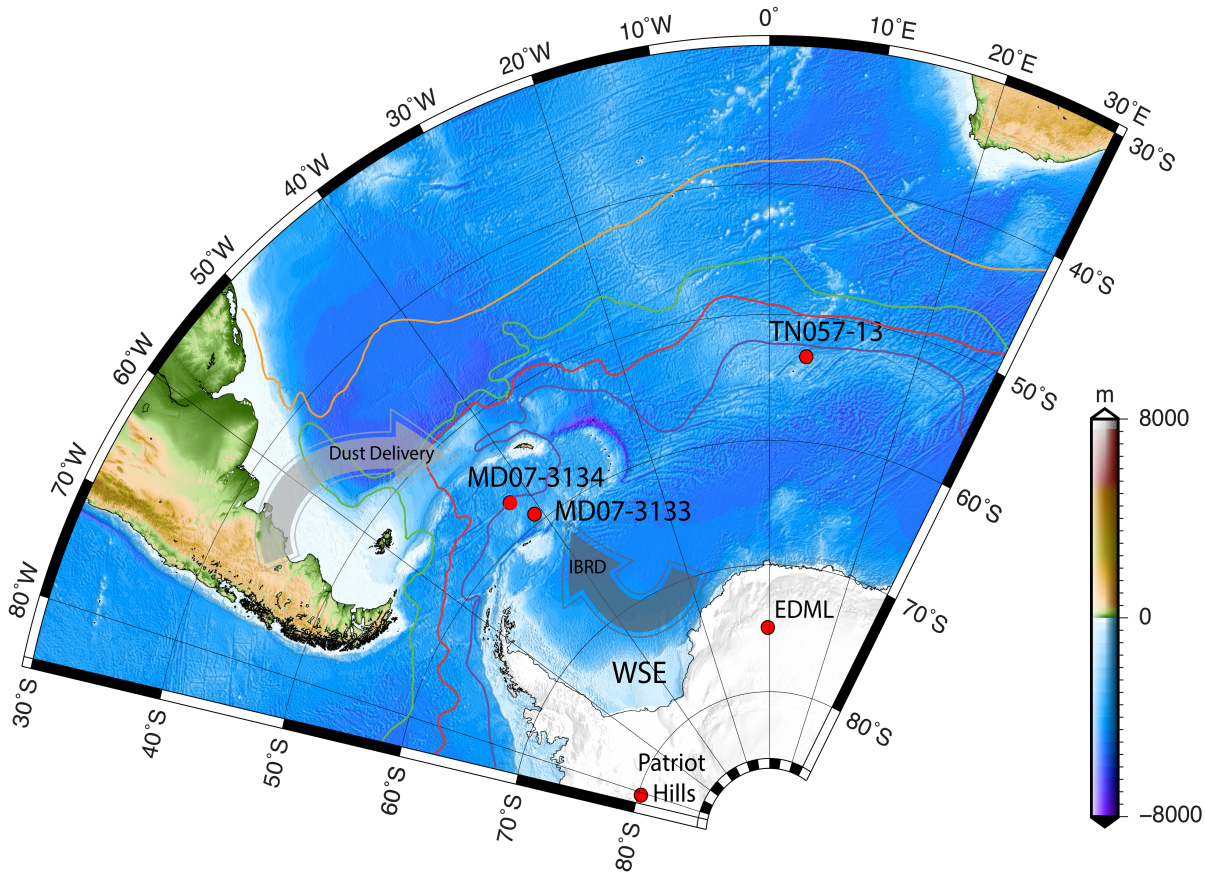

Figure 2. Location map of the South Atlantic sector of the Southern Ocean with the locations of Patriot Hills in the Ellsworth Mountains, the EPICA Dronning Maud Land (EDML) ice core (Wolff et al., 2006a), the Scotia Sea MD07-3134 core (Weber et al., 2014), and marine core TN057-13 (Anderson et al., 2009) produced with GMT (Wessel, 1998). Locations of the southern limb of the Antarctic Circumpolar Current (purple), the polar front (red), subantarctic front (green) and the subtropical front (yellow) (Orsi et al., 1995).

Changes in Southern Ocean productivity polewards of TN057-13 are recorded within the highly-resolved marine core MD07-3134, located at ~59°S in the Scotia Sea (Figure 1E; see Supplementary Information) (Weber et al., 2014). In common with core TN057-13 this sequence is exceptionally well resolved , with sedimentation rates of 20 to 200 cm/kyr (Weber et al., 2014). Here we report opal burial rates from MD07-3134 used, after accounting for sediment focussing with ^{230}Th normalisation (see Supplementary Information) (Meyer-Jacob et al., 2014), we estimate changes in biological productivity (export production) at the site (Figure 1E). The reconstruction suggests that whilst export production in the high-latitude Southern Ocean similarly increased from ~17 ka, the trend was maintained through the ACR, in antiphase to records further north (Anderson et al., 2009) (Figure 1 and Figure 2), suggesting that at high latitudes other driver(s) of marine biological activity may have operated during this period. In the absence of a network of highly resolved marine records from the high-latitude Southern Ocean that have been normalised for sedimentation rate changes (through ^{230}Th normalisation (see Supplementary Information)) (Sprenk et al., 2013), we develop a new record of high-latitude surface ocean productivity using the marine biomarkers and DNA analyses of picoplankton and nanoplankton from a highly-resolved horizontal ice core from the Weddell Sea Embayment, Antarctica (Fogwill et al., 2017), that captures regional-scale processes operating across the south Atlantic sector of the Southern Ocean across the LGT (Figure 3) (Fogwill et al., 2017; Turney et al., 2013).

Materials and methods

The 'horizontal' ice core record was obtained from the exposed blue ice area (BIA) at Patriot Hills in Horseshoe Valley, Ellsworth Mountains (Figure 2) (Fogwill et al., 2017), which, in contrast to many other BIA areas has not been mixed through ice flow (Fogwill et al., 2017; Winter et al., 2016a). Horseshoe Valley is a locally-sourced compound glacier that is buttressed by, but

ultimately coalesces with, the Institute Ice Stream close to the contemporary grounding line of the AIS making it the ideal site to build up a record of environmental and ice sheet change in this sector of Antarctica (Fogwill et al., 2017). With contemporary snow accumulation at the site being associated with low-pressure systems that have either tracked across the Weddell Sea from the southern Atlantic Ocean, or that relate to blocking by the Antarctic Peninsula (Abram et al., 2007; Reijmer et al., 1999; Turney et al., 2013), the site is ideally placed to record environmental changes across the Scotia Sea, Weddell Sea and high-latitude South Atlantic (Figure 2).

The Patriot Hills record is chronologically constrained by multiple greenhouse gas species (CO_2, CH_4 and N_2O) supported by geochemically identified volcanic (tephra) horizons (Figure 3 and Supplementary Information), with increased sampling and more tephra's identified providing tighter chronological control through the LGT building on previous studies (Fogwill et al., 2017). The age model demonstrates that the BIA sequence spans from ~2.5 to 50 kyr BP, with two unconformities (Discontinuities D1 and D2), that mark the build-up to (D1), and deglaciation from (D2), the last glacial cycle (Figure 3) (Fogwill et al., 2017). High-resolution ground penetrating radar (Winter et al., 2016b) and detailed analysis of trace gases and volcanic tephra horizons (Fogwill et al., 2017) demonstrates that the conformable BIA layers or 'isochrons' between these two unconformities span the period between ~11 to ~23 kyr BP (Figure 3C). Thus the horizontal ice core captures a unique highly-resolved record of ice-sheet dynamics (Fogwill et al., 2017), in an area of exceptionally slow moving ice, with no chronological breaks or unconformities across the LGT (see Supplementary Information), providing an opportunity to obtain large volume ice samples of known ages for innovative multiproxy biomarker analyses (Fogwill et al., 2017).

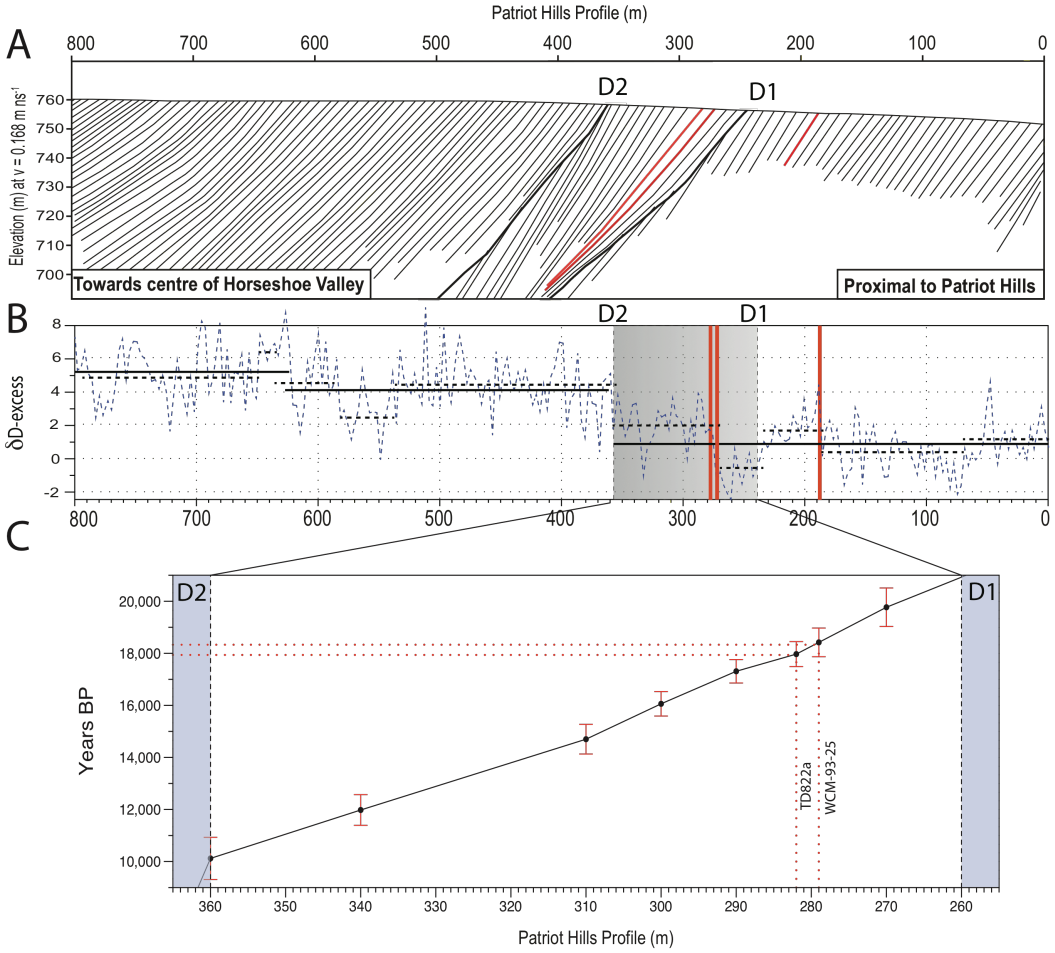

Figure 3. A. Schematic stratigraphic succession from Ground Penetrating Radar (GPR), across the Patriot Hills BIA, indicating ice accumulation punctuated by two periods of erosion (D1 and D2; thick black lines), and the position of tephras at 282m, 279m and 190m (red lines) across the profile (Fogwill et al., 2017). B. Dashed blue line represents δD-excess across profile; solid horizontal black lines denote potential regime shifts across the profile at 99% confidence, and dashed black lines denote potential regime shifts across the profile at 95% confidence (Rodionov, 2004). C. Age-depth model based upon chronological control ties between D1 ~21 ka (21,000 years) and D2 ~10 ka (10,000 years) as defined from volcanic 'tephra' horizons and most-likely age as derived from multiple trace gas comparison (CH_4, CO_2, N_2O; see Supplementary Information (Fogwill et

al., 2017)).

To examine regional environmental responses through the LGT, fluorescent organic matter (fOM) content and liquid chromatography organic carbon detection (LC-OCD) (Huber et al., 2011) analysis of biomarkers was undertaken on LGT ice outcropping at the Patriot Hills BIA (see Supplementary Information and Figure 4) (Huber et al., 2011). Detailed analysis of the fluorescence emission spectra identified two protein-like components (Stedmon et al., 2003) in ice throughout the profile. Due to their excitation-emission wavelengths, we can unambiguously identify these fOM components as those widely reported in precipitation as TRYLIS and TYLIS: tryptophan and tyrosine-like substances (Jørgensen et al., 2011; Parlanti et al., 2000) (see Supplementary Information (Figure S2)). Whilst there are limited studies in ancient Antarctic ice (D'Andrilli et al., 2016), past studies have demonstrated that a strong TRYLIS signal is found in Antarctic snow and ice derived from precipitation from the marine environment (Barker et al., 2013; Hood et al., 2009; King et al., 2019; Rohde et al., 2008; Smith et al., 2017).

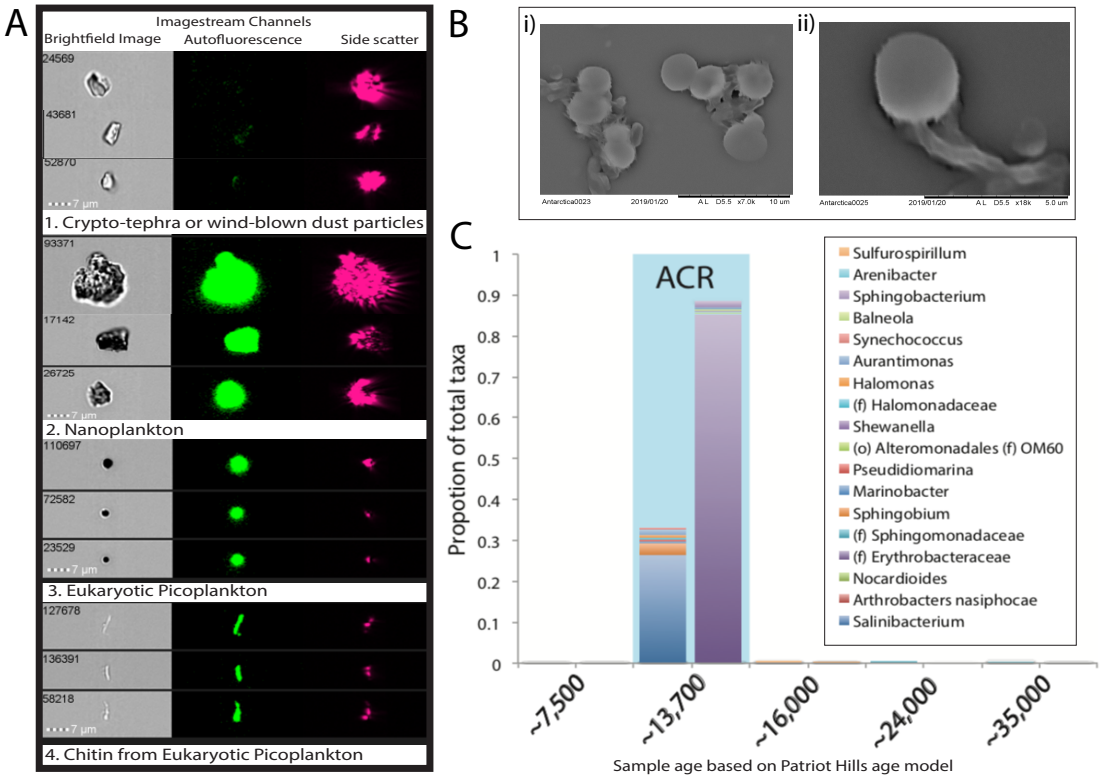

Figure 4. A. Imaging Flow Cytometry (ImageSteam®) analysis highlights the four principal populations identified in ancient ice from the Patriot Hills BIA. **B.** SEM images of marine picoeukaryotes with tails (chitin) **C.** Microorganisms previously identified in marine seawater (teal) or marine sediments (light blue) are observed in samples from different sections of the Patriot Hills BIA. The proportion of the taxa from each core, given a specific extraction method (Powerlyzer left hand side, or CTAB, right hand side). The period defined by the ACR is represented by the blue box.

To unambiguously identify the source of the fOM signal and confirm our interpretation of a marine origin we apply Imaging Flow Cytometry (ImageSteam®) and Scanning Electron Microscopy (SEM) to ancient ice samples. Imaging Flow Cytometry reveals four significant populations preserved within ice from samples in the Patriot Hills BIA record (Figure 4A). The first is an

255 inorganic fraction ranging from ~2-10μm in length, characterised by a flaky flat structure and no
256 autofluorescence, which we interpret as a mixture of crypto-tephra, and / or wind-blown dust. The
257 second population is composed of dark angular particles ~5-12μm in length, that have a high
258 autofluorescence, and a 3-D structure evidenced from a strong ch006 (side scatter) signal, which
259 we classify as nanoplankton. The third population is characterised by spheroidal forms ranging in
260 diameter from ~2-5μm, that again have a high autofluorescence, and a 3-D structure evidenced
261 from a strong ch006 (side scatter) signal, which we identify as Eukaryotic picoplankton and
262 picoeukaryotes. Finally, a fourth population is characterised by elongate spicules or rods between
263 2-10μm, that have a high autofluorescence, and a 3-D structure evidenced from a strong ch006
264 (side scatter) signal, which we identify as Chitin, most likely related to the third population of
265 eukaryotic picoplankton and picoeukaryotes, an interpretation confirmed through SEM (Figure
266 4B). Beyond these four populations only a few other events were recorded, which were identified
267 as broken diatom frustules, which were characterised by a high autofluorescence, and a side scatter
268 signal (see Supplementary Information).
269
270 Of the populations identified through Imaging Flow Cytometry (ImageSteam®) the eukaryotic
271 picoplankton and picoeukaryotes and Chitin populations made up most the made ~56% of the total,
272 with the non-fluorescent signal ~12%, and finally ~36% of the signal being less than <2μm,
273 therefore unclassified at present (Classification of this fine particulate fraction is difficult due to
274 its small size. However, ~20 % of events within this fraction are characteristic of picoeukaryotes
275 (displaying similar properties to eukaryotic picoplankton identified in the > 2 μm fraction, below).
276 The remaining 80 % is comprised of 'elongate fluorescent rods' (likely chitin), and unclassified
277 angular and round particulate.

278

279 The fact that the picoplankton and picoeukaryotes populations (>2μm) were not recorded as one
280 population in the Imaging Flow Cytometry (ImageSteam®) analysis was concerning, and likely
281 reflects the process of the flow cytometry, where sheath fluids run through the machine at the same
282 time as the sample – this focuses the sample in a steady stream, so that each 'event' can be analysed
283 individually. This effect, or possibly vortexing prior to analysis, may have disaggregated the
284 picoplankton and picoeukaryotes, separating the tails (chitin) from the spheroidal 'body' (see
285 Supplementary Information). To test this Scanning Electron Microscopy (SEM) was undertaken
286 on samples that had not been previously unfrozen or analysed. SEM imaging demonstrated
287 unambiguously that whole picoplankton and picoeukaryotes were present in the water samples
288 from ancient ice, complete with chitin (Figure 4B).

289

290 Having undertaken four independent yet mutually supportive biomarker approaches on ice samples
291 across the LGT from the Patriot Hills BIA we can conclude that marine biomarkers are present
292 throughout the profile. The location of the BIA, the unambiguous nature of the biomarker signal,
293 and the observation that marine regions have exceptionally low humic-like substances (HULIS)
294 content and relatively high TRYLIS content (Muller et al., 2008; Willey, 2000), indicates that the
295 primary source of fOM in the ice is from precipitation derived from the high-latitude Southern
296 Ocean (Abram et al., 2007; Reijmer et al., 1999; Turney et al., 2013). This interpretation is
297 supported by both independent LC-OCD and independent fluorescence techniques (see Figure 4
298 and Supplementary Information (Figure S2)), which fail to identify the presence of humic-like
299 substances in ice from the Patriot Hills BIA, ruling out either a terrestrial source of the fOM signal
300 or *in situ* secondary production(Smith et al., 2017) in the ancient ice which was recovered from

301 depth. Imaging Flow Cytometry (ImageSteam®) identifies that the bulk of the fOM signal relates
302 to the presence of microscopic marine plankton, principally picoplankton and picoeukaryotes, but
303 also with nanoplankton populations up to ~8μm in size.
304
305 As recorded in contemporary mesoscale experiments picoplankton and picoeukaryotes form the
306 basis of the pelagic communities response to iron fertilisation in the high-latitude HLNC Southern
307 Ocean(Boyd et al., 2000), and are key to CO_2 draw down in the polar Southern Ocean(Boyd et al.,
308 2019). With Imaging Flow Cytometry and independent biomarker (fOM and LC-OCD) analysis
309 demonstrating that the TRYLIS and TYLIS components identified are a measure of picoplankton
310 and picoeukaryotes populations the fOM signal can be interpreted as a robust measure of Southern
311 Ocean productivity in the Weddell and Scotia Sea areas of the South Atlantic sector of the Southern
312 Ocean. With both the TRYLIS and TYLIS components being identified in the WAIS Divide
313 core(Rohde et al., 2008) and in the fOM signal in contemporary snow cores from the Patriot Hills
314 site that record the past decade (see Supplementary Information (Figures S1and S2)), it provides a
315 measure of high-latitude surface marine productivity in this sector of the Southern Ocean that can
316 be linked to export production in the Southern Ocean (Boyd et al., 2000), a hypothesis testable
317 through the analysis of marine sediments from sites such as The Scotia Sea.
318
319 **Results**
320 By comparing the records of fOM across the LGT we observe a pronounced peak in these
321 biomarkers across the well-constrained ACR part of the Patriot Hills BIA sequence (Figure 5).
322 This change in fOM signal could reflect marked changes in precipitation source over the LGT;
323 however, regime shift analysis (Rodionov, 2004) on the deuterium-excess profile measured across

the LGT profile reveals no significant variability across the ACR, or the LGT, at either 99% or 95% confidence, indicating that the precipitation source remained constant (Figure 3C). The implication is that the fOM signal reflects large relative variations in the concentration of TRYLIS and TYLIS in the precipitation source region produced by the aerial transport of marine microorganisms, principally nanoplankton, picoplankton and picoeukaryotes as identified through ImageSteam®. In our analysis, we focus on the variation in the TRYLIS component, which makes up highest percentage of the variance in fOM signal (83.33%: see Supplementary Information). The fOM TRYLIS component, hence concentration of marine-derived nanoplankton, picoplankton and picoeukaryotes, is highly variable across the BIA ice core record but has a sustained high concentration through the ACR (Figure 5E).

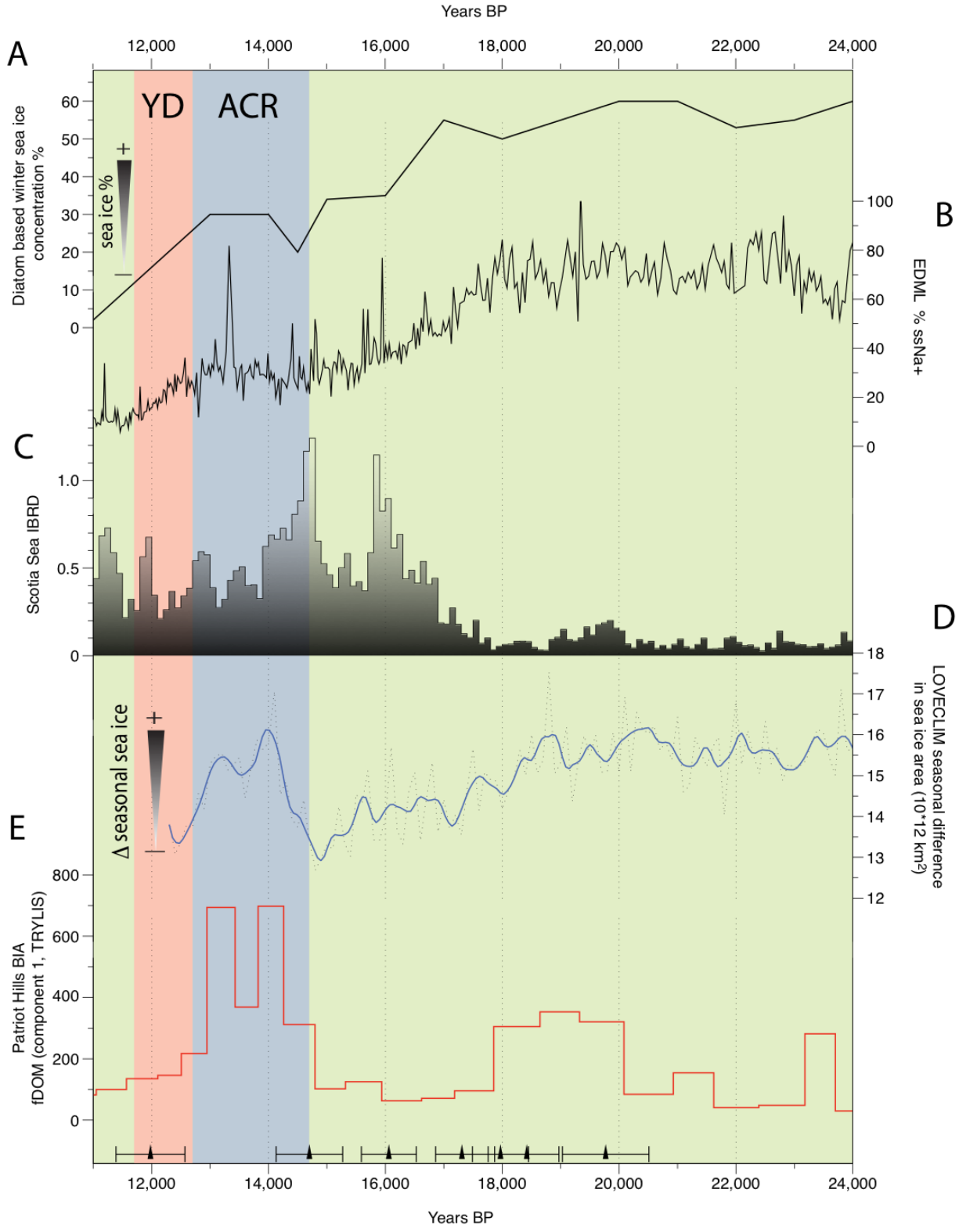
Years BP
12,000
14,000
16,000
18,000
20,000
22,000
24,000
A
YD
ACR
Diatom based winter sea ice concentration %
sea ice %
B
EDML % ssNa+
C
Scotia Sea IBRD
D
LOVECLIM seasonal difference in sea ice area (10*12 km2)
E
Δ seasonal sea ice
Patriot Hills BIA
fDOM (component 1, TRYLIS)

334

335 **Figure 5.** Comparison of A. Diatom transfer function-based estimates of winter sea-ice
336 concentration (Esper and Gersonde, 2014), B. Sea salt (ssNa+) from EPICA Dronning Maud Land
337 (EDML) (Wolff et al., 2006a). C. Iceberg-rafted debris flux (IBRD; normalised 100-year average)
338 relative to Holocene from core MD07-3134 (Weber et al., 2014). D. Difference in seasonal extent
339 of Antarctic sea-ice area from LOVECLIM (Menviel et al., 2011) and E. fOM concentration
340 (Component 1; TRYLIS, raw data is represented by a solid red line). Vertical boxes indicate the
341 periods defined by the Antarctic Cold Reversal (ACR) (blue), the Younger Dryas (YD)
342 chronozone (11.7-12.7 ka) and black triangles represent the age tie points (derived from
343 geochemically identified volcanic horizons and trace gases, see Supplementary Information and
344 Figure S1) in this section of the Patriot Hills BIA (see Figure 3).
345
346 To further investigate the detail of the marine biomarker signals, large volume ice samples were
347 sampled across the LGT portion of the exposed BIA at Patriot Hills to extract ancient bacterial
348 DNA *in situ* by directly melting and filtering samples from specific time-horizons – a novel
349 approach to minimize the introduction of contaminants (see Supplementary Information) and
350 which enables us to obtain insights into the picoplankton, picoeukaryotes and nanoplankton
351 represented at a taxa level. 16S rRNA indexing reveals a marked ecological switch characterized
352 by the appearance of large numbers of halotolerant microorganisms commonly found in seawater
353 was observed during the ACR, coincident with the increase in fOM TRYLIS signal (Figure 4C
354 (see Supplementary Information (Tables S1 and S2)). Specifically, we found marine-associated
355 taxa, *Helicobacteracea, Rhodobacteraceae, Marinobacter* and *Pseudidiomarina*, statistically
356 associated with the ACR period (p<0.038), and observe a slight increase in species diversity
357 (predominantly marine taxa) compared to that observed during either the mid-Holocene or the

358 glacial samples from the Patriot Hills BIA sequence (Figure 5, Tables S1 and S2). Whist the source
359 of this signal could have been from brine pools associated with the build-up of sea ice, we suggest,
360 based on the taxa identified, that the signal reflects an enhanced diversity and productivity from
361 open marine, or marginal sea ice zone. With five independent approaches (LC-OCD, Imaging
362 Flow Cytometry analysis, and the independent fOM and DNA) each pointing to enhanced marine
363 biological productivity in the high latitude South Atlantic sector of the Southern Ocean our results
364 infer that the ACR was a period of enhanced marine biological productivity. With the enhanced
365 picoplankton and picoeukaryotes signals derived from the surface precipitation source waters of
366 the HNLC Southern Ocean during the ACR, we suggest that there was a strengthening of the
367 biological pump which mirrored the effects of iron-fertilisation(Boyd et al., 2000) in this South
368 Atlantic Sector of the Southern Ocean, a finding that supports the enhanced export production
369 recorded in marine sediments from the Scotia Sea (Figure 1E) (Weber et al., 2014).
370

371 **Discussion**

372 To reconcile the apparent conflict between the increase in marine productivity recorded in marine
373 sediments from the Scotia Sea and the Patriot Hills ice core with the decrease reported further
374 north in the South Atlantic (Anderson et al., 2009; Jaccard et al., 2016) during the ACR, we
375 compare our record of marine biomarkers (fOM) captured in ice with potential drivers of Southern
376 Ocean productivity. We compare available records of iceberg rafted debris (IBRD; a proxy for
377 Antarctic iceberg discharge) (Weber et al., 2014)), sea salt sodium ($ssNa^{+}$) from the EDML ice
378 core (a proxy for sea-ice extent) (Wolff et al., 2006b), proxy sea-ice reconstructions (Abelmann et
379 al., 2015; Esper and Gersonde, 2014) to investigate possible physical drivers of enhanced
380 productivity, and we compare independent transient modelling experiments using LOVECLIM

that include fresh water hosing in the Ross and Weddell seas (Menviel et al., 2011) (Figure 5; and Supplementary Information). Comparison between these records and the BIA LGT record between ~24 and ~14.6 kyr BP indicate weak relationships between marine biological productivity (using opal flux as a measure of export production), sea-ice expansion, atmospheric CO_2 variability and the peak in marine derived biomarkers (fOM), agreeing with previous studies (Figure 5) (Collins et al., 2012). This contrasts with the period defined by the ACR, where we observe a strong relationship between marine fOM in the Patriot Hills BIA, increased production of biogenic opal in the Scotia Sea, and the extended atmospheric CO_2 plateau across the ACR (Figures 1 and 5). Given that this increase in marine productivity seen in the Scotia Sea during the ACR is not apparent in mid-latitude marine records (Figure 2)(Anderson et al., 2009; Jaccard et al., 2016), we focus on possible high-latitude drivers of CO_2 exchange: iron fertilization from enhanced IBRD flux (Duprat et al., 2016), a reduction in Antarctic Bottom Water (AABW) formation due to enhanced freshwater flux (Fogwill et al., 2015; Golledge et al., 2014; Menviel et al., 2010), and sea-ice feedbacks (Abelmann et al., 2015) (Figure 6).

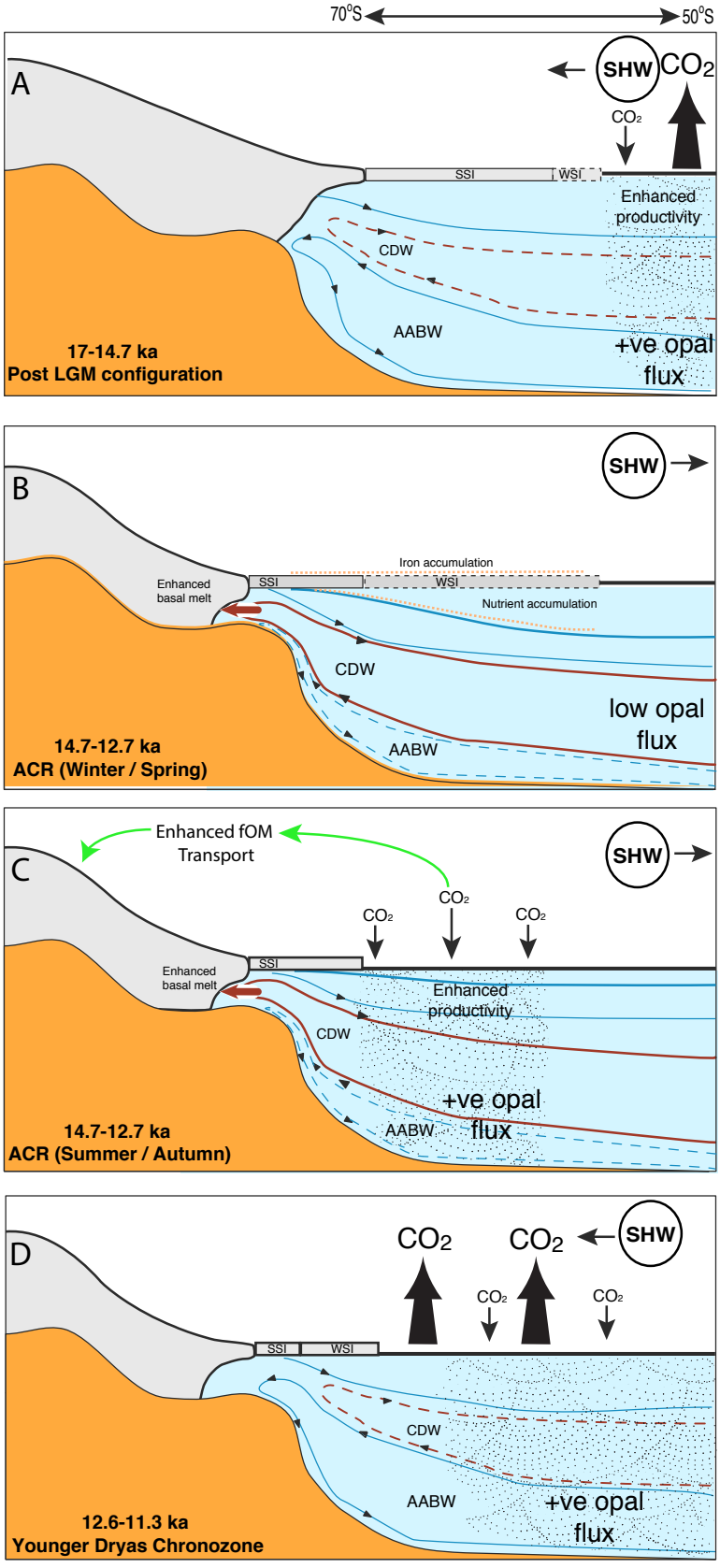
70°S
50°S
A
SHW
CO2
CO2
SSI
WSI
Enhanced productivity
CDW
AABW
+ve opal flux
17-14.7 ka
Post LGM configuration
B
SHW
Iron accumulation
Enhanced basal melt
SSI
WSI
Nutrient accumulation
CDW
low opal flux
AABW
14.7-12.7 ka
ACR (Winter / Spring)
C
Enhanced fOM Transport
SHW
CO2
CO2
CO2
SSI
Enhanced basal melt
Enhanced productivity
CDW
+ve opal flux
AABW
14.7-12.7 ka
ACR (Summer / Autumn)
D
CO2
CO2
SHW
CO2
CO2
SSI
WSI
CDW
AABW
+ve opal flux
12.6-11.3 ka
Younger Dryas Chronozone

396 **Figure 6.** Schematic cross section of the mid to high latitude Southern Ocean. A. Post-Last Glacial
397 Maximum (LGM) configuration with southerly displacement of the Southern Hemisphere
398 Westerlies (SHW), depicting enhanced overturning of mid-latitude Southern Ocean between ~17
399 ka- 14.7 ka as suggested by opal flux (Anderson et al., 2009). B. Antarctic Cold Reversal with
400 enhanced intrusion of Circumpolar Deepwater (CDW) onto Antarctic shelf areas. Austral winter /
401 spring, depicts marked winter sea-ice expansion (WSI), northwards migration of the SHW, with
402 stratification and deepening of the mixed layer allowing 'nutrient refuelling' from deeper nutrient-
403 enriched ocean and reduction in AABW formation at high-latitudes (Abelmann et al., 2015). C.
404 Antarctic Cold Reversal (austral summer/autumn), extensive WSI break up enhancing marine
405 primary productivity, from light and iron fertilization in a warming ocean leading to enhanced CO_2
406 drawdown in high-latitude HNLC Southern Ocean. D. Younger Dryas chronozone mid-latitude
407 overturning reinvigorated leading to degassing of old carbon, and enhanced opal flux across the
408 Southern Ocean.
409
410 IBRD contains high concentrations of bioavailable iron, making iceberg melt a potential source
411 for increased primary productivity and carbon sequestration through fertilization across the HNLC
412 regions of the high-latitude Southern Ocean (Duprat et al., 2016). Intriguingly, despite significant
413 evidence for potential enhanced iron fertilization of the Southern Ocean through increased delivery
414 of IBRD at around 20-19 kyr BP and 17-16 kyr BP (Weber et al., 2014), there does not seem to be
415 a strong biological response in the Patriot Hills fOM or Scotia Sea opal flux records (Figures 2 and
416 5), suggesting enhanced IRBD influx did not lead to enhanced high-latitude marine export
417 production.
418

Alternatively, an increase in meltwater flux and reduction in the rate of AABW formation during the ACR (Golledge et al., 2014; Menviel et al., 2011; Menviel et al., 2016; Weber et al., 2014) may have increased stratification and carbon sequestration across the high-latitude Southern Ocean. Published analysis has demonstrated that there was significant ice-sheet drawdown across the Weddell Sea Embayment at this time (Fogwill et al., 2017; Weber et al., 2014), suggesting that influx of meltwater could have triggered stratification, and substantial circulation changes across the broader Southern Ocean, magnified by associated shifts in the intensity and/or location of surface westerly air flow (Anderson et al., 2009; Fogwill et al., 2017; Hogg et al., 2016; Jaccard et al., 2016). This interpretation is supported by independent ice-sheet and Earth system modelling experiments (Menviel et al., 2011; Weber et al., 2014). However, the disparity in the opal flux records between marine cores from the mid-latitude South Atlantic (Anderson et al., 2009) and Scotia Sea, suggests that the enhanced export production was focussed on the high-latitude South Atlantic during the ACR (Figure 1).

An alternative mechanism that could enhance marine productivity at the high-latitudes involves sea-ice feedbacks. Recent studies of full glacial conditions suggest that reduced surface–deep ocean exchange and enhanced nutrient consumption by phytoplankton in the Southern Ocean may have lowered atmospheric CO_2 (Abelmann et al., 2015; Collins et al., 2012). During the austral winter, sea-ice expansion allowed the mixed layer to deepen, 'refuelling' the surface ocean with nutrients from the deep ocean reservoir, and enhancing near-surface productivity and export production during the break up of sea ice in the subsequent summer. This process was likely amplified by the addition of iron from sea-ice melt and breakup in the post-glacial HNLC ocean, and possibly seasonal temperature changes and $CaCO_3$ dissolution (Delille et al., 2014).

442

443 The strong marine fOM signal preserved in the Patriot Hills BIA coincides with Southern
444 Hemisphere surface ocean and atmosphere cooling during the ACR (Figure 5). Proxy records and
445 transient Earth system modelling (Menviel et al., 2011) suggest the highest seasonal variability in
446 sea-ice extent across the LGT took place during the ACR (with greatest extent during winter and
447 spring) (Figure 5), implying these sea-ice feedbacks were amplified across this period (Figure 6).
448 The conditions contrast markedly in the periods immediately prior to (Figure 6A) and following
449 (Figure 6D) the ACR, when the seasonal sea ice zone was relatively less variable (Figure 5), the
450 high-latitude Southern Ocean less stratified (Golledge et al., 2014; Menviel et al., 2011; Weber et
451 al., 2014), and the location of the Intertropical Convergence Zone (ITCZ) and mid-latitude
452 Southern Hemisphere Westerlies were relatively further south (Figure 2). Set against a backdrop
453 of a warming ocean during the LGT this likely created ideal conditions for enhanced Southern
454 Ocean productivity in the high-latitude Southern Ocean, especially in sectors of the South Atlantic
455 such as the Weddell and Scotia seas.

456

457 Comparison between our continuous Scotia Sea opal flux record (Weber et al., 2014) and the
458 Patriot Hills BIA fOM record suggests that we are capturing a high-latitude signal of enhanced
459 surface marine primary productivity caused by marked seasonal sea-ice variability during the
460 ACR, a period characterised by a sustained atmospheric CO_2 plateau (Jaccard et al., 2016; Marcott
461 et al., 2014; Schmitt et al., 2012). During the ACR, most marine records across the mid-latitudes
462 suggest the biological pump in the Southern Ocean weakened, in apparent contradiction of the
463 plateau in atmospheric CO_2 at that time (Figure 2). Our results indicate that despite low dust input
464 (Figure 2), and surface cooling across subantarctic waters during the ACR, marked variability in

sea-ice extent resulted in increased seasonal surface productivity in the HNLC waters of the high-latitude South Atlantic sector of the Southern Ocean in comparison to periods prior to and following this event (Figure 5). We suggest that increased seasonal marine primary productivity in fact enhanced the Southern Ocean organic carbon pump, increasing carbon drawdown (and leading to enhanced export production) (Figure 6). Whilst other mechanisms may have played a part in the 1,900 year-long ACR CO_2 plateau – including iron fertilization, cool Southern Ocean surface temperatures and possibly reductions in the rate of AABW formation – the potential that seasonal Southern Ocean sea-ice feedbacks in the South Atlantic sector of the high-latitude Southern Ocean may have contributed to a slowdown in the rate of CO_2 rise during the ACR is a significant observation that has implications for our understanding of the role of the Southern Ocean in global carbon dynamics. Crucially, our results imply that during periods of Southern Ocean sea-ice expansion, high variability in winter and summer sea-ice extent may result in enhanced carbon sequestration as seen recently , providing a negative feedback during periods of rising CO_2, a finding that requires detailed assessment given contemporary Antarctic sea ice changes (Barnes, 2015).

Acknowledgments: CJF, CSMT, LM, NRG, LSW and AC are supported by their respective Australian Research Council (ARC) and Royal Society of NZ fellowships, and CJF and AC thanks Keele University for a Research Development Award that underpinned this research at Keele University ICELAB and Exeter University. Fieldwork was undertaken under ARC Linkage Project (LP120200724), supported by Linkage Partner Antarctic Logistics and Expeditions whose support we gratefully acknowledge. CSIRO's contribution was supported in part by the Australian Climate Change Science Program (ACCSP), an Australian Government Initiative. SMD acknowledges

488 financial support from Coleg Cymraeg Cenedlaethol and the European Research Council (ERC
489 grant agreement no. 25923). MEW acknowledges support from the Deutsche
490 Forschungsgemeinschaft (grant We2039/8-1). The data reported in this paper are archived on the
491 NOAA Paleoclimatology website. There are no competing interests.

492

493 **Author contribution:** CJF, CSMT, AB and AC conceived this research. CJF, CSMT, AB, MEW,
494 DE, MR DPT, TDvO, ADM, MAJC, SD, MB, NCM, JV, AR, LM, HM, CM, JY, MM, AC, MH,
495 AP, JL, LSW and AC undertook analysis and sampling. CJF, CSMT, AB, MEW and AC wrote
496 the manuscript with input from all the authors.

497

498 **Data availability:** The Patriot Hills δd and $\delta^{18}O$ isotope data, and the age model is available at
499 National Oceanic and Atmospheric Administration Paleoclimatology Database
500 (https://www.ncdc.noaa.gov/paleo/study/21691), and the data from core MD07-3134 are available
501 at http://dx.doi.org/10.1594/PANGAEA.819646. The biomarker and DNA data will be made
502 available upon publication through the NOAA archive.

503

504 **Additional Information:**

505 The authors declare no competing interests. Supplementary information accompanies this paper at
506 www.xxxxxxx. Correspondence and requests for materials should be addressed to C.J.F.
507 c.j.fogwill@keele.ac.uk.

508

509

510

References

Abelmann, A., Gersonde, R., Knorr, G., Zhang, X., Chapligin, B., Maier, E., Esper, O., Friedrichsen, H., Lohmann, G., Meyer, H., and Tiedemann, R., 2015, The seasonal sea-ice zone in the glacial Southern Ocean as a carbon sink: Nature Communications, v. 6, p. 8136.

Abram, N. J., Mulvaney, R., Wolff, E. W., and Mudelsee, M., 2007, Ice core records as sea ice proxies: An evaluation from the Weddell Sea region of Antarctica: Journal of Geophysical Research, v. 112, no. D15101.

Anderson, R. F., Ali, S., Bradtmiller, L. I., Nielsen, S. H. H., Fleisher, M. Q., Anderson, B. E., and Burckle, L. H., 2009, Wind-Driven Upwelling in the Southern Ocean and the Deglacial Rise in Atmospheric CO2: Science, v. 323, no. 5920, p. 1443-1448.

Barker, J. D., Dubnick, A., Lyons, W. B., and Chin, Y.-P., 2013, Changes in Dissolved Organic Matter (DOM) Fluorescence in Proglacial Antarctic Streams: Arctic, Antarctic and Alpine Research, v. 45, no. 3, p. 305-317.

Barnes, D. K. A., 2015, Antarctic sea ice losses drive gains in benthic carbon drawdown: Current Biology, v. 25, no. 18, p. R789-R790.

Bauska, T. K., Baggenstos, D., Brook, E. J., Mix, A. C., Marcott, S. A., Petrenko, V. V., Schaefer, H., Severinghaus, J. P., and Lee, J. E., 2016, Carbon isotopes characterize rapid changes in atmospheric carbon dioxide during the last deglaciation: Proceedings of the National Academy of Sciences, v. 113, no. 13, p. 3465-3470.

Boyd, P. W., Claustre, H., Levy, M., Siegel, D. A., and Weber, T., 2019, Multi-faceted particle pumps drive carbon sequestration in the ocean: Nature, v. 568, no. 7752, p. 327-335.

Boyd, P. W., Watson, A. J., Law, C. S., Abraham, E. R., Trull, T., Murdoch, R., Bakker, D. C. E., Bowie, A. R., Buesseler, K. O., Chang, H., Charette, M., Croot, P., Downing, K., Frew, R., Gall, M., Hadfield, M., Hall, J., Harvey, M., Jameson, G., LaRoche, J., Liddicoat, M., Ling, R., Maldonado, M. T., McKay, R. M., Nodder, S., Pickmere, S., Pridmore, R., Rintoul, S., Safi, K., Sutton, P., Strzepek, R., Tanneberger, K., Turner, S., Waite, A., and Zeldis, J., 2000, A mesoscale phytoplankton bloom in the polar Southern Ocean stimulated by iron fertilization: Nature, v. 407, p. 695.

Butterworth, B. J., and Miller, S. D., 2016, Air-sea exchange of carbon dioxide in the Southern Ocean and Antarctic marginal ice zone. : Geophysical Research Letters, v. 43, p. 7223-7230.

Collins, L. G., Pike, J., Allen, C. S., and Hodgson, D. A., 2012, High-resolution reconstruction of southwest Atlantic sea-ice and its role in the carbon cycle during marine isotope stages 3 and 2: Paleoceanography, v. 27, no. 3, p. PA3217.

D'Andrilli, J., Foreman, C. M., Sigl, M., Priscu, J. C., and McConnell, J. R., 2016, A 21,000 year record of organic matter quality in the WAIS Divide ice core: Clim. Past Discuss., v. 2016, p. 1-15.

Delille, B., Vancoppenolle, M., Geilfus, N.-X., Tilbrook, B., Lannuzel, D., Schoemann, V., Becquevort, S., Carnat, G., Delille, D., Lancelot, C., Chou, L., Dieckmann, G. S., and Tison, J.-L., 2014, Southern Ocean CO2 sink: The contribution of the sea ice: Journal of Geophysical Research: Oceans, v. 119, no. 9, p. 6340-6355.

Duprat, L. P. A. M., Bigg, G. R., and Wilton, D. J., 2016, Enhanced Southern Ocean marine productivity due to fertilization by giant icebergs: Nature Geosci, v. 9, p. 219-221.

559 Esper, O., and Gersonde, R., 2014, New tools for the reconstruction of Pleistocene Antarctic sea
560 ice: Palaeogeography, Palaeoclimatology, Palaeoecology, v. 399, p. 260-283.
561 Fogwill, C., Turney, C., Golledge, N., Etheridge, D., Rubino, M., Thornton, D., Baker, A.,
562 Woodward, J., Winter, K., and Van Ommen, T., 2017, Antarctic ice sheet discharge
563 driven by atmosphere-ocean feedbacks at the Last Glacial Termination: Scientific reports,
564 v. 7, p. 39979.
565 Fogwill, C. J., and Kubik, P. W., 2005, A glacial stage spanning the Antarctic Cold Reversal in
566 Torres del Paine (51 degrees S), Chile, based on preliminary cosmogenic exposure ages:
567 Geografiska Annaler Series a-Physical Geography, v. 87A, no. 2, p. 403-408.
568 Fogwill, C. J., Phipps, S. J., Turney, C. S. M., and Golledge, N. R., 2015, Sensitivity of the
569 Southern Ocean to enhanced regional Antarctic ice sheet meltwater input: Earth's Future,
570 v. 3, no. 10, p. 317-329.
571 Golledge, N. R., Menviel, L., Carter, L., Fogwill, C. J., England, M. H., Cortese, G., and Levy,
572 R. H., 2014, Antarctic contribution to meltwater pulse 1A from reduced Southern Ocean
573 overturning: Nat Commun, v. 5.
574 Gottschalk, J., Skinner, L. C., Lippold, J., Vogel, H., Frank, N., Jaccard, S. L., and Waelbroeck,
575 C., 2016, Biological and physical controls in the Southern Ocean on past millennial-scale
576 atmospheric CO2 changes.: Nat Commun, v. 7, no. 11539.
577 Hewitt, A. J., Booth, B. B. B., Jones, C. D., Robertson, E. S., Wiltshire, A. J., Sansom, P. G.,
578 Stephenson, D. B., and Yip, S., 2016, Sources of uncertainty in future projections of the
579 carbon cycle.: Journal of Climate, v. 29, p. 7203-7213.
580 Hogg, A., Southon, J., Turney, C., Palmer, J., Bronk Ramsey, C., Fenwick, P., Boswijk, G.,
581 Friedrich, M., Helle, G., Hughen, K., Jones, R., Kromer, B., Noronha, A., Reynard, L.,
582 Staff, R., and Wacker, L., 2016, Punctuated shutdown of Atlantic Meridional Overturning
583 Circulation during the Greenland Stadial 1: Scientific Reports, v. 6, no. 25902.
584 Hood, E., Fellman, J., Spencer, R. G. M., Hernes, P. J., Edwards, R., D/'Amore, D., and Scott,
585 D., 2009, Glaciers as a source of ancient and labile organic matter to the marine
586 environment: Nature, v. 462, no. 7276, p. 1044-1047.
587 Huber, S. A., Balz, A., Abert, M., and Pronk, W., 2011, Characterisation of aquatic humic and
588 non-humic matter with size-exclusion chromatography – organic carbon detection –
589 organic nitrogen detection (LC-OCD-OND): Water Research, v. 45, no. 2, p. 879-885.
590 Jaccard, S. L., Galbraith, E. D., Martínez-García, A., and Anderson, R. F., 2016, Covariation of
591 deep Southern Ocean oxygenation and atmospheric CO2 through the last ice age: Nature,
592 v. 530, p. 207-210.
593 Jaccard, S. L., Hayes, C. T., Martínez-García, A., Hodell, D. A., Anderson, R. F., Sigman, D. M.,
594 and Haug, G. H., 2013, Two Modes of Change in Southern Ocean Productivity Over the
595 Past Million Years: Science, v. 339, no. 6126, p. 1419-1423.
596 Jørgensen, L., Stedmon, C. A., Kragh, T., Markager, S., Middelboe, M., and Søndergaard, M.,
597 2011, Global trends in the fluorescence characteristics and distribution of marine
598 dissolved organic matter: Marine Chemistry, v. 126, no. 1, p. 139-148.
599 King, A., Wolff, E., Thomas, E., Kalberer, M., Giorio, C., and MargitSchwikowski, 2019, Novel
600 organic compounds in ice cores for use in paleoclimatereconstruction: Geophysical
601 Research Abstracts, , v. EGU General Assembly 2019, no. CL1.11/CR5.6
602 Le Quéré, C., Rödenbeck, C., Buitenhuis, E. T., Conway, T. J., Langenfelds, R., Gomez, A.,
603 Labuschagne, C., Ramonet, M., Nakazawa, T., Metzl, N., Gillett, N., and Heimann, M.,

2007, Saturation of the Southern Ocean CO2 sink due to recent climate change. : Science, v. 316, p. 1735-1738.

Marcott, S. A., Bauska, T. K., Buizert, C., Steig, E. J., Rosen, J. L., Cuffey, K. M., Fudge, T. J., Severinghaus, J. P., Ahn, J., Kalk, M. L., McConnell, J. R., Sowers, T., Taylor, K. C., White, J. W. C., and Brook, E. J., 2014, Centennial-scale changes in the global carbon cycle during the last deglaciation: Nature, v. 514, no. 7524, p. 616-619.

Marshall, J., and Speer, K., 2012, Closure of the meridional overturning circulation through Southern Ocean upwelling. : Nature Geoscience, v. 5, p. 171-180.

Martínez-García, A., Sigman, D. M., Ren, H., Anderson, R. F., Straub, M., Hodell, D. A., Jaccard, S. L., Eglinton, T. I., and Haug, G. H., 2014, Iron Fertilization of the Subantarctic Ocean During the Last Ice Age: Science, v. 343, no. 6177, p. 1347-1350.

McGlone, M. S., Turney, C. S. M., Wilmshurst, J. M., Renwick, J., and Pahnke, K., 2010, Divergent trends in land and ocean temperature in the Southern Ocean over the past 18,000 years: Nature Geosci, v. 3, no. 9, p. 622-626.

Menviel, L., A. Timmermann, O. Elison Timm, and Mouchet, A., 2011, Deconstructing the Last Glacial Termination: the role of millennial and orbital-scale forcings: Quaternary Science Reviews, v. 30, p. 1155-1172.

Menviel, L., J. Yu, F. Joos, A. Mouchet, K. J. Meissner, and England, M. H., 2016, Poorly ventilated deep ocean at the Last Glacial Maximum inferred from carbon isotopes: A data-model comparison study.: Paleoceanography, v. 31.

Menviel, L., Timmermann, A., Timm, O. E., and Mouchet, A., 2010, Climate and biogeochemical response to a rapid melting of the West Antarctic Ice Sheet during interglacials and implications for future climate: Paleoceanography, v. 25, no. 4, p. PA4231.

Meyer-Jacob, C., Vogel, H., Boxberg, F., Rosén, P., Weber, M., and Bindler, R., 2014, Independent measurement of biogenic silica in sediments by FTIR spectroscopy and PLS regression: Journal of Paleolimnology, v. 52, no. 3, p. 245-255.

Monnin, E., Inderm√ºhle, A., D√§llenbach, A., Fl√ºckiger, J., Stauffer, B., Stocker, T. F., Raynaud, D., and Barnola, J.-M., 2001, Atmospheric CO2 Concentrations over the Last Glacial Termination: Science, v. 291, no. 5501, p. 112-114.

Muller, C. L., Baker, A., Hutchinson, R., Fairchild, I. J., and Kidd, C., 2008, Analysis of rainwater dissolved organic carbon compounds using fluorescence spectrometry. : Atmospheric Environment, v. 34, p. 8036-8045.

Orsi, A. H., III, T. W., and W. D. Nowlin, J., 1995, On the meridional extent and fronts of the Antarctic Circumpolar Current,: Deep-Sea Research, v. 1, no. 42, p. 641-673.

Parlanti, E., Wörz, K., Geoffroy, L., and Lamotte, M., 2000, Dissolved organic matter fluorescence spectroscopy as a tool to estimate biological activity in a coastal zone submitted to anthropogenic inputs: Organic Geochemistry, v. 31, no. 12, p. 1765-1781.

Pedro, J. B., Bostock, H. C., Bitz, C. M., He, F., Vandergoes, M. J., Steig, E. J., Chase, B. M., Krause, C. E., Rasmussen, S. O., Markle, B. R., and Cortese, G., 2015, The spatial extent and dynamics of the Antarctic Cold Reversal: Nature Geosci, v. 9, p. 51-55

.

Reijmer, C. H., Greuell, W., and Oerlemans, J., 1999, The annual cycle of meteorological variables and the surface energy balance on Berkner Island, Antarctica,: Ann. Glaciol., v. 29, p. 49-54.

649 Rodionov, S. N., 2004, A sequential algorithm for testing climate regime shifts: Geophys. Res.
650 Lett., v. 31, no. L09204.
651 Rohde, R. A., Price, P. B., Bay, R. C., and Bramall, N. E., 2008, In situ microbial
652 metabolism as a cause of gas anomalies in ice: Proceedings of the National Academy of
653 Sciences, v. 105, no. 25, p. 8667-8672.
654 Schmitt, J., Schneider, R., Elsig, J., Leuenberger, D., Lourantou, A., Chappellaz, J., Köhler, P.,
655 Joos, F., Stocker, T. F., Leuenberger, M., and Fischer, H., 2012, Carbon Isotope
656 Constraints on the Deglacial CO2 Rise from Ice Cores: Science, v. 336, no. 6082, p. 711-
657 714.
658 Smith, H. J., Foster, R. A., McKnight, D. M., Lisle, J. T., Littmann, S., Kuypers, M. M. M., and
659 Foreman, C. M., 2017, Microbial formation of labile organic carbon in Antarctic glacial
660 environments: Nature Geosci, v. 10, no. 5, p. 356-359.
661 Sprenk, D., Weber, M. E., Kuhn, G., Rosén, P., Frank, M., Molina-Kescher, M., Liebetrau, V.,
662 and Röhling, H.-G., 2013, Southern Ocean bioproductivity during the last glacial cycle –
663 new decadal-scale insight from the Scotia Sea: Geological Society, London, Special
664 Publications, v. 381, no. 1, p. 245-261.
665 Stedmon, C. A., Markager, S., and Bro, R., 2003, Tracing dissolved organic matter in aquatic
666 environments using a new approach to fluorescence spectroscopy.: Marine Chemistry, v.
667 82, p. 239–254.
668 Toggweiler, J. R., Russell, J. L., and Carson, S. R., 2006, Midlatitude westerlies, atmospheric
669 CO2, and climate change during the ice ages: Paleoceanography, v. 21, no. 2.
670 Turney, C. S. M., Fogwill, C. J., Van Ommen, T. D., Moy, A. D., Etheridge, D., Rubino, M.,
671 Curran, M. A. J., and A., R., 2013, Late Pleistocene and early Holocene change in the
672 Weddell Sea: a new climate record from the Patriot Hills, Ellsworth Mountains, West
673 Antarctica: Journal of Quaternary Science, v. 28, no. 7, p. 697-704.
674 Turney, C. S. M., Palmer, J., Hogg, A., Fogwill, C. J., Jones, R. T., Bronk Ramsey, C., Fenwick,
675 P., Grierson, P., Wilmshurst, J., O'Donnell, A., Thomas, Z. A., and Lipson, M., 2016,
676 Multidecadal variations in Southern Hemisphere atmospheric 14C: Evidence against a
677 Southern Ocean sink at the end of the Little Ice Age CO2 anomaly: Global
678 Biogeochemical Cycles, v. 30, no. 2, p. 211-218.
679 Weber, M. E., Clark, P. U., Kuhn, G., Timmermann, A., Sprenk, D., Gladstone, R., Zhang, X.,
680 Lohmann, G., Menviel, L., Chikamoto, M. O., Friedrich, T., and Ohlwein, C., 2014,
681 Millennial-scale variability in Antarctic ice-sheet discharge during the last deglaciation:
682 Nature, v. 510, no. 7503, p. 134-138.
683 Wessel, P. a. S., W.H., , 1998, New, improved version of Generic Mapping Tools released.: Eos,
684 Transactions American Geophysical Union, v. 79, no. 47, p. 579-579.
685 Willey, J. D., Kieber, R.J., Eyman, M.S., Avery Jr., G.B., 2, 2000, Rainwater dissolved organic
686 carbon: concentrations and global flux. : Global Biogeochemical Cycles, v. 14, p. 139–
687 148.
688 Winter, K., Woodward, J., Dunning, S. A., Turney, C. S., Fogwill, C. J., Hein, A. S., Golledge,
689 N. R., Bingham, R. G., Marrero, S. M., and Sugden, D. E., 2016a, Assessing the
690 continuity of the blue ice climate record at Patriot Hills, Horseshoe Valley, West
691 Antarctica: Geophysical Research Letters, v. 43, no. 5, p. 2019-2026.
692 Winter, K., Woodward, J., Dunning, S. A., Turney, C. S. M., Fogwill, C. J., Hein, A. S., Golledge,
693 N. R., Bingham, R. G., Marrero, S. M., Sugden, D. E., and Ross, N., 2016b, Assessing the

694 continuity of the blue ice climate record at Patriot Hills, Horseshoe Valley, West
695 Antarctica: Geophys. Res. Lett., v. 10.1002/2015GL066476.
696 Wolff, E., Fischer, H., Fundel, F., Ruth, U., Twarloh, B., Littot, G., Mulvaney, R., Rothlisberger,
697 R, d. A., M, , Boutron, C., Hansson, M., Jonsell, U., Hutterli, M., Lambert, F., Kaufmann,
698 P., Stauffer, B., Stocker, T., Steffensen, J., Bigler, M., Siggaard-Andersen, M., Udisti, R.,
699 Becagli, S., Castellano, E., Severi, M., Wagenbach, D., Barbante, C., Gabrielli, P., and
700 Gaspari, V., 2006a, Southern Ocean sea-ice extent, productivity and iron flux over the
701 past eight glacial cycles. : Nature, v. 440, p. 491-496.
702 Wolff, E. W., Fischer, H., Fundel, F., Ruth, U., Twarloh, B., Littot, G. C., Mulvaney, R.,
703 Röthlisberger, R., de Angelis, M., Boutron, C. F., Hansson, M., Jonsell, U., Hutterli, M.
704 A., Lambert, F., Kaufmann, P., Stauffer, B., Stocker, T. F., Steffensen, J. P., Bigler, M.,
705 Siggaard-Andersen, M. L., Udisti, R., Becagli, S., Castellano, E., Severi, M., Wagenbach,
706 D., Barbante, C., Gabrielli, P., and Gaspari, V., 2006b, Southern Ocean sea-ice extent,
707 productivity and iron flux over the past eight glacial cycles: Nature, v. 440, no. 7083, p.
708 491-496.
709

710

711

712

713

714

715

716

717

718

719

720